Fusion Engineering and Design 123 (2017) 669–673

Contents lists available at ScienceDirect

Fusion Engineering and Design

journal homepage: www.elsevier.com/locate/fusengdes

Response of the imaging cameras to hard radiation during JET operation

Alexander Huber[a,*], Gennady Sergienko[a], David Kinna[b], Valentina Huber[c], Alberto Milocco[b,d], Laurent Mercadier[b], Itziar Balboa[b], Sean Conroy[e], Simon Cramp[b], Vasili Kiptily[b], Uron Kruezi[b], Horst Toni Lambertz[a], Christian Linsmeier[a], Guy Matthews[b], Sergey Popovichev[b], Philippe Mertens[a], Scott Silburn[b], Klaus-Dieter Zastrow[b], JET contributors[1]

[a] Forschungszentrum Jülich GmbH, Institut für Energie- und Klimaforschung – Plasmaphysik, Partner of the Trilateral Euregio Cluster (TEC), 52425 Jülich, Germany
[b] CCFE, Culham Science Centre, Abingdon, OX14 3DB, UK
[c] Forschungszentrum Jülich GmbH, Supercomputing Centre, 52425 Jülich, Germany
[d] University of Milano Bicocca, Piazza della Scienza 3, 20126 Milano, Italy
[e] Department of Physics and Astronomy, Uppsala University, Uppsala, Sweden

HIGHLIGHTS

- The camera image sensors degrade with time mainly due to neutron radiation damage.
- Cooling the sensor down to −20 °C essentially reduced the effects of the radiation damage; no detectable degradation of the actively cooled sensors has been observed.
- Uncooled cameras must be replaced once/year after neutron fluence ~1.9–3.2 × 10^{12} n/cm^2.
- The generation of a significant amount of dynamic hot pixels was observed in the presence of hard radiation.
- Failure of the electronics at fluence ~2–4.0 × 10^9 n/cm^2.

ARTICLE INFO

Article history:
Received 29 September 2016
Received in revised form 30 March 2017
Accepted 30 March 2017
Available online 8 April 2017

Keywords:
CCd
Camera
Radiation damage
Hot pixels
Image
Camera cooling

ABSTRACT

The analysis of the radiation damage of imaging systems is based on all different types of analogue/digital cameras with uncooled as well as actively cooled image sensors in the VIS/NIR/MWIR spectral ranges. The Monte Carlo N-Particle (MCNP) code has been used to determine the neutron fluence at different camera locations in JET. An explicit link between the sensor damage and the neutron fluence has been observed. Sensors show an increased dark-current and increased numbers of hot-pixels. Uncooled cameras must be replaced once per year after exposure to a neutron fluence of ~1.9–3.2 × 10^{12}neutrons/cm^2. Such levels of fluence will be reached after ≈14-22 ELMy H-mode pulses during the future D-T campaign. Furthermore, dynamical noise seen as a random pattern of bright pixels was observed in the presence of hard radiation (neutrons and gammas). Failure of the digital electronics inside the cameras as well as of industrial controllers is observed beyond a neutron fluence of about ~4 × 10^9 neutrons/cm^2. The impact of hard radiation on the different types of electronics and possible application of cameras during future D-T campaign is discussed.

1. Introduction

In magnetic fusion devices of the next generation such as ITER, high neutron and gamma-ray yields could be detrimental to the applied diagnostic equipment such as video imaging systems as well as to electronic components of machine control systems. Semiconductor devices are particularly sensitive to the radiation, both

* Corresponding author.
E-mail address: A.huber@fz-juelich.de (A. Huber).
[1] See the Appendix of F. Romanelli et al., Proceedings of the 25th IAEA Fusion Energy Conference 2014, Saint Petersburg, Russia.

http://dx.doi.org/10.1016/j.fusengdes.2017.03.167

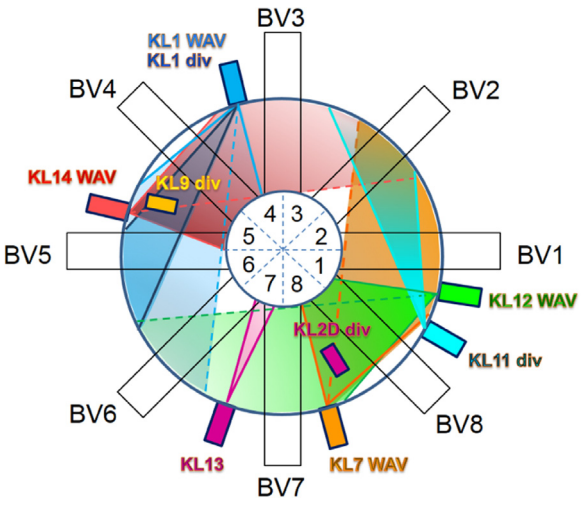

Fig. 1. Top view of the JET tokamak. Fields of View (FoV) of protection NIR CCD cameras. KL1 div, KL11 div, KL2D and KL14 have 2 cameras for each view.

ionizing (formation of traps at the Si/SiO2 interface with energy levels within the silicon bandgap) and non-ionizing (displacement damage effects) [1]. Defects degrade the performance of CCD image sensors by increasing the average dark-current and dark-current non-uniformity, which result in the appearance of individual pixels with high dark-currents ("hot-pixels"). The effects of radiation in CMOS sensors are similar to CCD in that both suffer from ionising radiation and displacement damage [2]. In this contribution, we would like to summarize the experience of camera operation acquired during the D-D experimental campaigns on the JET.

2. Experimental details

The analysis of the radiation damage of imaging systems is based on all different types of cameras:

- 4 operations cameras, colour CCD (Cohu DSP 3600 Series 3611) with uncooled as well as actively cooled image sensors (sensor: Sony ICX419AKL, pixel size: 8.6 μm (H) × 8.3 μm (V) [3])
- 13 protection near-infrared (NIR) CCD cameras (Hitachi KP-M1AP; sensor: Sony ICX423AL pixel size: 11.6 μm (H) × 11.2 μm (V) [3])
- 7 scientific digital CCD cameras (Allied Vision Technologies (AVT) Pike F–100 B [4]) in near ultraviolet and visible (NUV/VIS) wavelength range with uncooled as well as actively cooled image sensors (sensor:KAI–1020 M, pixel size: 7.4 μm × 7.4 μm [4])
- 4 mid-wave infrared (MWIR) CMOS cameras with actively cooled (78 K) image InSb sensors: ISC9705 (320 × 256) with pixel size 30 μm × 30 μm and ISC9803 (640 × 512) with pixel size 25 μm × 25 μm [5]).

The cameras are mostly located at the top of the machine as well as at the equatorial plane and distributed across the different octants (see Fig. 1 for the location of the protection NIR CCD cameras on JET).

Additionally, the impact of hard radiation on the different types of electronics such as electronics inside cameras, frame grabbers, PLC (Programmable Logic Controller) control units will be discussed in this contribution.

Neutron transport calculations have been performed using the MCNP6 code (Monte Carlo N-Particle [6]) in order to determine the neutron flux/fluence at different locations in the JET tokamak, using an advanced JET model. JET biological shield and penetrations as well as all significant components such as major diagnostics were modelled in detail. Simulations were performed for D-D toroidal plasma discharge sources with Gaussian-shaped neutron energy spectrum with peak energy of E_c = 2.5 MeV and the FWHM = 16.6 keV. The neutron flux [n/cm^2 per source neutron] was calculated as an average over a void 10 cm side square box centred at the nominal position of each CCD camera. To keep the statistical error of the simulations below 5% the code used relatively large numbers of source neutrons, in the order of 6×10^9. The neutron flux was then scaled by the total neutron yield during JET campaigns to obtain the neutron fluence [neutrons/cm^2] at locations of each JET cameras. The neutron yield for any JET discharge of the campaign was evaluated by a set of fission chambers, which represent the primary neutron measurement [7,8].

It is common practise to characterize the neutron fluence from a source in terms of an equivalent monoenergetic neutron fluence. The 1 MeV Silicon equivalent fluence was evaluated according to the ASTM guide E722-09 [9]. The neutron fluence, calculated with MCNP6 as described above, was multiplied by the displacement damage function (tabulated in [9]), the product integrated between 0 and 20 MeV and divided by the reference value of the damage function at 1 MeV.

3. Radiation effects on camera sensors

3.1. Hot spot pixel definition and identification

When pixels are damaged by radiation, they can suffer enhanced dark current and they appear to be much brighter than surrounding pixels. Such pixels are called hot pixels. In this study, the identification of the hot spots was performed by application of a second-order derivative edge detection filter to the image. The aim of this application is to emphasize the regions of rapid intensity change. The Laplacian is used here for edge detection [10] and the hot pixels have been defined by selection of pixels where the signal exceeds a certain threshold. This threshold is chosen as 5–6 σ, where σ is the standard deviation of the image for new cameras before installation on the JET machine.

The pixel size of the camera sensor is an important parameter with respect to radiation damage. From our experience we know that the sensors with smaller pixel sizes suffer more radiation damage. Also the exposure time can impact on the damage level: the number of hot spots increases with exposure time.

3.2. Impact of the radiation on the uncooled cameras

It should be distinguished between the damage to individual images, which only occurs during radiation with production of the dynamic hot pixels which appear temporarily only during the neutron/gammas exposures and image effects resulting from permanent damage of image sensors after heavy radiation. The latter results in the generation of static hot pixels which remain over time. To investigate the impact of the radiation on the CCD, a digital camera type AVT Pike 100 B with uncooled sensor was installed in the JET Torus Hall. The camera was fixed on the KL1 endoscope in Octant 4 and was oriented in toroidal direction. "Dark" exposures of the camera during the JET operations with closed lens cap for detection of dark current noise and hot pixels have been applied. The camera was operated with 1 Mega Pixel resolution at a bit rate of 8 bits with an exposure time of 20 ms.

3.2.1. Permanent damage of the camera sensor

Fig. 2 shows the evolution of the AVT pike camera background image (raw data) during the time period from 21/02/2009 to 23/10/2009. The total number of neutrons produced over this time period is 2.93×10^{19} neutrons corresponding to the neutron fluence in the area of camera location of $\sim 1.2 \times 10^{12}$ neutrons/cm^2. At

Fig. 2. Evolution of the AVT Pike 100B camera background image with the radiation exposure time.

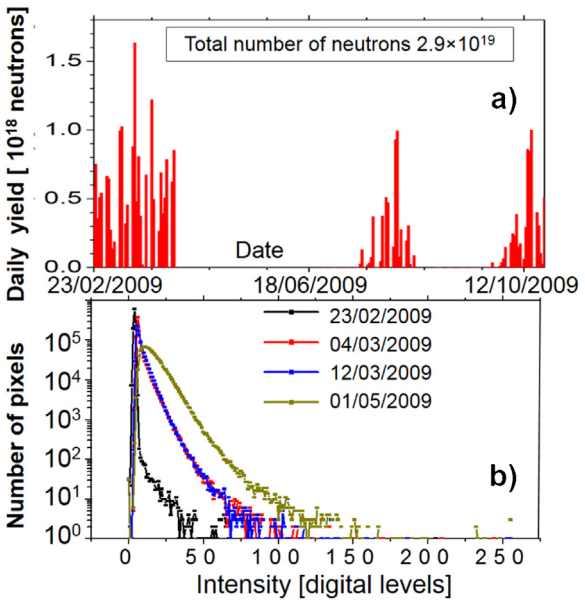

Fig. 3. a) the daily neutron yield during the testing period b) histograms of pixel brightness at four selected times during the test.

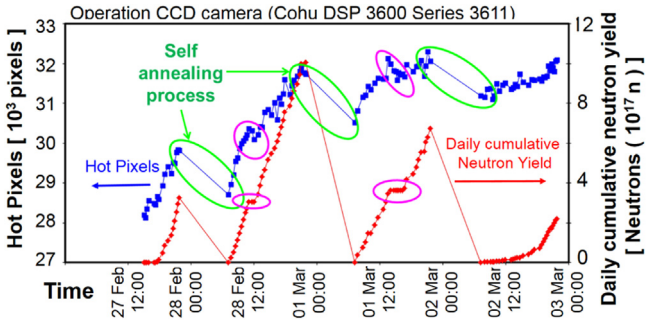

Fig. 4. Evolution of hot pixels on the sensor of the operation of uncooled camera as function of the daily neutron yield.

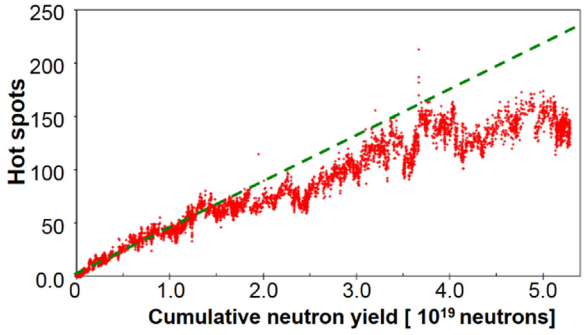

Fig. 5. Hot spots as function of cumulative neutron yield on the uncooled camera used for operation.

the beginning the image shows only a little number of the bright pixels which increase during the test. At the end of the test period, the camera suffered from serious radiation damage which can be seen by numerous bright pixels (static hot pixels) randomly distributed across the entire sensor. Fig. 3a shows the daily neutron yield during the reported test period. The yield strongly depends on the experimental program which was carried out on JET during this time. Additionally, Fig. 3b shows histograms of pixel brightness during the testing time. The image sensors show an accumulative degradation due to radiation damage: increase of the pixels average dark level, increase of standard deviation of the dark level and the increased number of static "hot" pixels which are saturated (see Fig. 3b). Fig. 4 shows the evolution of hot pixels of one of the operation colour CCD camera (Cohu DSP 3600 Series 3611) with uncooled sensor as function of the total neutron yield accumulated during the four consecutive days of experiments. The daily cumulative neutron yield is always zero at the beginning of a day, because the first pulse is usually a dry run, with no neutron emitted. The observation shows that the number of hot pixels behave the same way as the cumulated number of neutrons. We can see that the number of hot pixels is higher for the last pulse of one day than for the first pulse of the following experimental day. Additionally, during non-operating periods (marked by green cycles) the numbers of the hot spots are reduced exhibiting the self-annealing of the camera. Primary defects produced during the radiation exposure are not stable. Interstitials and vacancies are mobile at room temperature causing partial annealing of defects. This effect is also called beneficial annealing [11]. Please note that the daily gamma dose is proportional to the daily neutron yield.

The JET cameras are exposed simultaneously to both neutrons and gammas, the individual impact of which cannot be distinguished. However, there are experiments where cameras have been shielded against the neutrons by a 5% boron doped polyethylene composite (with a thickness of 10 cm). The neutron adsorption in the shield material accompanies with consequent emission of gammas and we could investigate the footprint of induced hot pixels by neutrons and gammas separately. According to our observations the single neutrons impacted mostly a group of neighbouring pixels (2–3), what we call here the "hot spots" or the single "hot" pixel at saturated level. The gammas produce the single "hot" pixel with moderate intensity below the saturation level. The graph on Fig. 5 represents the hot spots of the uncooled operation camera (Cohu DSP 3600 Series 3611) against the cumulative neutron yield. The total number of neutrons 5.2×10^{19} produced over the time period

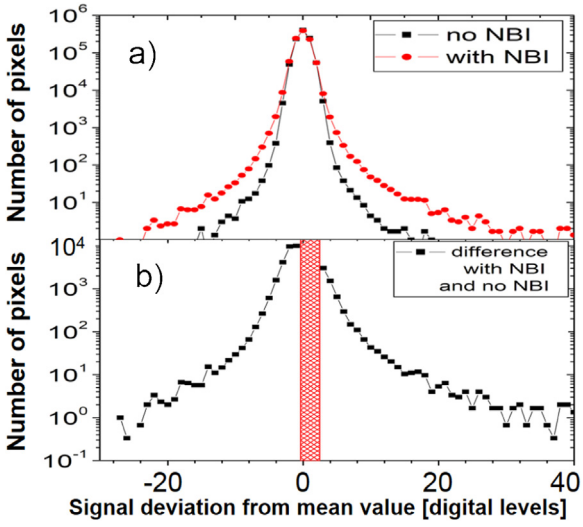

Fig. 6. a) Daynamical evolution of hot pixels during the NBI phase and during the ohmic phase of the typical JET 15 MW NBI plasma pulse. b) gives the difference between two distributions shown in Fig. 6a.

between 08/03/2006 and 21/02/2007 corresponds to a neutron fluence in the area of the camera location of $\sim 3.4 \times 10^{12}$ n/cm^2. We can see at the beginning a linear trend on the growth of hot pixels indicating the good correlation of the former quantity with the neutron fluence. The operation during this time period results in increased numbers of hot pixels as well as in an increased dark current making the further use of the camera impossible: about 10% pixels were affected by neutrons and gammas. Based on the JET experience, each operation camera must be replaced once/year after a neutron yield of $\approx 3–5 \times 10^{19}$ neutrons amounting to the neutron fluence $\sim 1.9–3.2 \times 10^{12}$ n/cm^2.

For the comparison of the JET result with other irradiation facilities, the characterization of neutron irradiation from the JET source in terms of 1 MeV Si equivalent fluence has been performed. The fluence of $\sim 1.9\text{-}3.2 \times 10^{12}$n/cm^2 from the JET source corresponds to $\sim 0.62\text{-}1.06 \times 10^{12}$ n/cm^2 Si equivalent fluence at 1 MeV. Such levels of fluence will be reached after ≈14-22 ELMy H-mode pulses [12] (ref. #74176, 4.5 MA/3.6 T, power of neutral beam heating $P_{NBI} = 25$ MW, $t_{NBI} = 6$s) during the future D-T campaign.

3.2.2. Temporary damage of the camera sensor

The generation of the dynamical hot pixels on the AVT Pike 100 B camera sensor during the exposure time has been clearly observed during the JET experiment. Fig. 6a shows the distributions of the cameras pixels as function of the intensity deviation from the mean value during the JET plasma phases with additional NBI heating (red curve) and during the pure ohmic heating alone. The last phase does not contribute to the neutron generation. During the NBI phase we observed nearly symmetrical distribution broadening indicating the creation of the dynamical hot pixels. Fig. 6b presents the difference between two distribution shown in Fig. 6a. The number of pixels with mean value (in the marked red region) have been reduced during the NBI phase. These pixels are redistributed over the profile shown in Fig. 6b. About 32700 pixels, 3% of the total amount of the sensor pixels, are temporarily affected by neutrons and gammas. Such a relatively large number of dynamical hot pixels requires an on-line software for their handling in real-time to avoid any wrong interpretation. Such software has been successfully integrated into the JET real-time protection system based on the video imaging recording [13,14].

3.3. Impact of the radiation on the cooled cameras

Based on the experience made with uncooled cameras discussed in Section 3.2, all scientific cameras (AVT) Pike F-100B) as well as operation cameras have been upgraded and operated since 2009 with actively cooled sensors and do not show any significant visible damage. It should be mentioned here that the temperature of the camera sensors is routinely monitored. Cooling a video sensor to −20 °C significantly reduces the dark current and eliminates “hot” pixels. Also, none of MWIR CMOS cameras with actively cooled (78 K) image sensors shows any signature of the radiation damages. The decreased leakage current of the pixels of the actively cooled cameras can be explained by the strong temperature dependence of the leakage current. In the defective pixels the temperature induced excitation of carriers increases the leakage current while the band structure of the semiconductor is changed and thermal hopping of charge carriers into the conduction band can occur. This thermal hooping can be avoided by cooling the sensor [15].

The cameras must be kept all the times in frozen conditions. Defrosting of the sensor leads to a partial recovery of the defects inside the sensor and, correspondingly, to an increase of the dark current and to the appearance of hot pixels. However, the number of recovered hot pixels is much less than the number of hot pixels in the camera operated with un-cooled sensor from the beginning. This behavior is related to reverse annealing where primary defects build up stable electrically active clusters. A similar observation has been reported in many contributions (for example in [16]). It is stated in [16] that irradiating CCDs at low temperature can produce different trap population than the same irradiation at warm temperature. Keeping the CCD cold at all times may prevent formation of certain types of defects and reduce the sensor damage.

The basic mechanisms of displacement damage and subsequent formation of electrically active defects have been summarized in [11,17]. The reactions between vacancies, interstitial and substitutional atoms is strongly temperature dependent leading to creation of different type of defect complexes under cold (below 0C) and warm (even at RT) conditions.

Based on these mechanisms Kono suggested the model [18] which explains the reverse annealing behavior after the room temperature bake-out.

4. Radiation effects on the electronics

Radiation produced during operation of JET could be detrimental to electronic components and systems used to control and to protect the JET machine. Especially, the first wall protection system [13] based on the imaging diagnostics requires fulfilling sharp demands that allow a reliable operation of the JET tokamak. Radiation could impact the electronics inside the cameras as well as the periphery electronic components responsible for the data capture and the control of the imaging system.

4.1. The impact of radiation on the camera electronics

Seven AVT Pike F-100B cameras with actively cooled sensors have been operated since 2010 [19]. This camera is a commercial product which contains semiconductor based components, such as a 32bit microcontroller and Numonyx^{TM} embedded flash memories, all of which are sensitive to neutrons [20]. It has been observed that the camera periodically terminated the FireWire connection with PC in the experiments when the NBI power exceeded 9 MW in a pure deuterium plasma. Once the connection was terminated, it was possible to run the camera again only by power-off-power-on cycling. Fig. 7 shows the numbers of losses of the FireWire connections as function of the cumulative total neutrons emit-

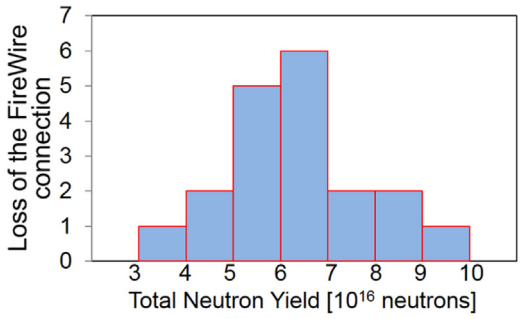

Fig. 7. Radiation effects on electronics of AVT Pike F100B cameras (FireWire connection).

ted during the time period between the power cyclings of the cameras. We can see that camera loses with high probability the connection with the PC when the total neutron yield reaches the value of about 6–7 $\times$ 10^{16} neutrons. The total number of 6–7 $\times$ 10^{16} neutrons corresponds to 3–4 pulses with P_{NBI} of about 20 MW and amounts to *n*-fluence in the area of the camera location of ~2.0–2.4 $\times$ 10^9 n/cm^2. The longest time period of camera operation without malfunction corresponds to a total number of 10^{17} neutrons.

Malfunction of the electronics of MWIR CMOS cameras most probably due to the impact onto the flash memory has been observed. Failure of the digital electronics inside the cameras requires the re-installation of the firmware software after a total yield of about 1.6 $\times$ 10^{18} n corresponding to about 1 month of operation and to a neutron fluence in the area around 4.3 $\times$ 10^9 n/cm^2.

4.2. The impact of radiation on the periphery electronics

The JET protection imaging system [13] contains 13 analog monochrome CCD cameras (HITACHI KP/M1AP) operating in the near infrared spectral region to measure the surface temperature of the plasma-facing components. Frame grabbers convert the analog output of the CCD cameras into a digital, 8-bit, Gigabit Ethernet signal. They are located inside the Torus Hall and suffer from exposure to the neutrons/gammas. A loss of the time vector has been observed with the frequency of once/month. The one month of operation amounts to a total neutron yield ≈2.7 $\times$ 10^{18}n and to a neutron fluence of ~0.4 $\times$ 10^{10} n/cm^2. The malfunction is probably due to impact of the neutrons onto the electronics inside of the module or due to false triggering affecting the optical reset signal.

On JET, the control of the scientific video system (control of the filter exchanger, camera cooling, sensor temperature monitoring) is based on the Simatic S7-PLC (Programmable Logic Controller) technique. The PLC is located inside the unshielded cubicle positioned on top of transformer iron in the JET Torus Hall. One time per month, the PLC PC loses the connection with the PLC module (corresponds to total neutron yield of about 2.8 $\times$ 10^{18} neutrons, fluence ~4.0 $\times$ 10^9 n/cm^2).

5. Summary

During the JET D-D campaign an obvious correlation between sensor damage and neutron fluence has been observed. There is a definitive impact on some image parameters, like an increased dark-current and increased numbers of hot-pixels. The operation of the cameras at room-temperature demonstrates a strong sensor damage which requires the camera replacement once per year after exposure to a neutron fluence of ~1.9–3.2 $\times$ 10^{12}n/cm^2. It was demonstrated that cooling sensors down to −20 °C can essentially reduce the effect of the radiation damage and increase the lifetime of the image sensor. Furthermore, the generation of a significant amount of dynamic hot pixels (≈3% the total amount of the sensor pixels) was observed in the presence of hard radiation (neutrons and gammas). Malfunction of the digital electronics inside the cameras, frame grabbers, as well as of industrial PLC controllers is observed beyond a neutron fluence of about ~4 $\times$ 10^9 n/cm^2 (corresponds to ~0.6-1.6 $\times$ 10^9 n/cm^2 equivalent silicon displacement fluence at 1 MeV)

Acknowledgments

This work has been carried out within the framework of the EUROfusion Consortium and has received funding from the Euratom research and training programme 2014–2018 under grant agreement No 633053. The views and opinions expressed herein do not necessarily reflect those of the European Commission.

References

[1] G.R. Hopkinson, Radiation-induced Dark Current Increases in CCDs, RADECS 93. Second European Conference on Radiation and Its Effects on Components and Systems (Cat. No.93TH0616-3), 1993 (St. Malo, p.401 10.1109/RADECS.1993.316569).
[2] N. Waltham, CMOS and CCD Sensors, ISSI SR-009, 2013, pp. 423–442 http://ankaa.unibe.ch/forads/sr-009-23.pdf.
[3] http://www.eureca.de/english/optoelectronics_sony.html.
[4] http://www.adept.net.au/cameras/avt/pdf/PIKE_F_100B_C.pdf.
[5] http://www.flir.de/cores/display/?id=51948.
[6] J.T. Goorley, et al., Initial MCNP6 Release Overview: MCNP6 Version 1.0, LANL Report LA-UR-13-22934, 2013.
[7] M.T. Swinhoe, O.N. Jarvis, Calculation and measurement of 235U and 238U fission counter assembly detection efficiency, Nucl. Instrum. Methods Phys. Res. 221 (2) (1984) 460–465, http://dx.doi.org/10.1016/0167-5087(84)90020-6 (ISSN 0167-5087).
[8] B.J. Laundy, et al., Fusion Technol. 24 (1993) 150.
[9] ASTM E722-09, Standard Practice for Characterizing Neutron Fluence Spectra in Terms of an Equivalent Monoenergetic Neutron Fluence for Radiation-Hardness Testing of Electronics, 2009.
[10] M. Juneja, P.S. Sandhu, International Journal of Computer Theory and Engineering 1 (5) (2009) 1793.
[11] R. Wunstorf, IEEE Trans. Nucl. Sci. 44 (1997) (p806).
[12] H. Zohm, Plasma Phys. Control. Fusion 38 (1996) 105.
[13] G. Arnoux, et al., Rev. Sci. Instrum. 83 (2012) 10D727.
[14] M. Jouve, et al., Preprint EFDA-JET-CP(11) 06/01, 2011.
[15] H. Spieler, et al., Semiconductor Detector Systems, OUP Oxford, 2005 (ISBN 978-0-19-852784-8).
[16] M. Bautz, et al., IEEE Trans. Nucl. Sci. 52 (2005) 519.
[17] V.A.J. Van Lint, Nucl. Instrum. Methods A253 (1987) 453.
[18] K. Kono, et al., SPIE Proceed. 4140 (2000) 267.
[19] A. Huber, et al., Rev. Sci. Instrum. 83 (2012) 10D511.
[20] K. Iniewsk, Radiation Effects in Semiconductors, CRC Press, 2010 (ISBN 9781439826942).